Innovation & Technology Advances, 2026, 4(1), 17-30
https://bergersci.com/index.php/jta/index
DOI: 10.61187/ita.v4i1.253

Optimal Design of Thermal Insulation Performance of Transport Packaging Box Based on Response Surface Algorithm

Yan Zhang[1,*], Ruchuan Shi[2]

[1]School of Information Engineering, Nanyang Institute of Technology, Nanyang, Henan, 473004, China
[2]College of Perception Science and Engineering, Shanghai Jiaotong University, Shanghai, 200240, China

*Correspondence: zhangyan@nyist.edu.cn

Abstract: On the premise of ensuring thermal insulation performance and structural strength, lightweight design of spacecraft transport packaging box is helpful to energy saving and emission reduction. In order to achieve this goal, based on the finite element analysis method of heat conduction process, the influence of design variables such as insulation layer size, material type and aluminum square tube size on the box performance is studied. The experimental scheme was designed by response surface method, and each scheme was simulated by Ansys Fluent. The obtained data were fitted by multiple quadratic regression to obtain the mapping relationship between each parameter and weight, and the optimal scheme was obtained through processing and analysis. The results show that the safety factor of the optimized box structure is 1.21, which meets the design requirements. After 4 hours, the internal temperature of the box is 23.86℃, which is lower than the external temperature of the box to meet the expected requirements, and the box quality is reduced by 13.3% compared with that before optimization. Through the application of response surface algorithm, the weight of the box is reduced to the greatest extent under the dual constraints of thermal insulation performance and structural strength, and the lightweight optimization design of the transportation packaging box is realized.

Keywords: Transport packing box; Thermal insulation performance; Response surface method; Material safety factor; Optimization design

How to cite this paper: Zhang, Y., Shi, R. Optimal Design of Thermal Insulation Performance of Transport Packaging Box Based on Response Surface Algorithm. Innovation & Technology Advances, 2026, 4(1), 17–30.
https://doi.org/10.61187/ita.v4i1.253

1. Introduction

The transportation packaging plays a crucial role in the transportation process of spacecraft, to ensure that the spacecraft is not adversely affected by external environmental temperatures during transportation, the design of the transportation packaging box is a complex engineering problem. Factors affecting the storage and transportation equipment of spacecraft mainly include temperature, humidity, pressure, airtightness, vibration, impact, etc [1-4].

Modern transportation increasingly emphasizes efficiency and energy conservation. Lightweight design, while meeting temperature and strength requirements, can reduce energy consumption and carbon emissions. Ensuring the safety, reliability, and insulation performance during the transportation process is crucial in spacecraft development. Significant progress has been made in the design and research of structural models for spacecraft transportation packaging boxes. Xiao Gang et al. [5] based their design of the bottom, lid, and shock absorption system on a certain model of air transport packaging box, using the results of air transport tests to demonstrate the rationality of the packaging box design. Su Xinming et al. [6] selected the polyurethane foam board with low thermal conductivity as the insulation layer material, using the Fourier law of heat conduction and safety factor

theory, and conducted fluid and heat transfer coupled calculations through Fluent software. They evaluated the passive insulation performance of the packaging box by transient solution method after modeling a certain spacecraft and packaging box. The analysis showed that the insulation performance inside the packaging box met the requirements. Singh et al. [7] evaluated insulation materials, box forms, and phase change materials, confirming that temperature-sensitive products must be kept within the appropriate temperature range during storage and transportation. Paquette et al. [8] verified a three-dimensional model of multi-layer box heat transfer, indicating that the parameters with the greatest influence on insulation performance are the thermal conductivity of the box walls and the inner surface reflectivity, while the heat transfer coefficient has a smaller impact on insulation performance. Rezgar et al. [9] proposed an effective model based on the gas-solid two-phase conductivity and radiative thermal conductivity for predicting the thermal conductivity of polymer foam materials, successfully obtaining the optimal solution through theoretical models and experimental results. Matsunaga et al. [10] utilized two mathematical calculation methods to propose a new concept of multi-temperature zone cold chain distribution and studied the effect of the cooling capacity inside the insulation box on the insulation effect under temperature conditions with periodic changes.

In recent years, research and development work on optimization methods to maximize or minimize one or more objective functions under various constraints has made certain progress. Liu Cuina et al. [11] found that combining vacuum insulation panels with polyurethane foam significantly improved the insulation effect of the packaging box, while increasing the thickness of the polyurethane foam layer optimized the internal structure of the insulation box without reducing the effective volume. Ao Feng et al. [12], while maintaining the stiffness and strength of the columns stable, established a finite element model of variable-section columns through structural stress analysis, and conducted lightweight design using response surface method, successfully reducing the overall weight by about 20%. Huang Dengfeng et al. [13] conducted stiffness and strength analysis on aluminum alloy lightweight materials used in box semi-trailers using Hyper Works software, screening factors in the variables, and conducting optimization design through the expandable grid sequence method and constructing an approximate model using the least squares method. Finally, adaptive response surface method was used to complete the optimization design. Wu Shuai et al. [14] based on ANSYS parameterized language APDL, optimized the structure size of a certain type of bucket wheel in order to minimize the overall volume, and established a parameterized model for bucket wheel stacker-reclaimers, achieving lightweight design. Liu et al. [15] proposed a two-stage optimization procedure for composite material wing design based on strength and buckling constraints, fitting a third-order polynomial response surface to the optimal buckling load in different angular directions, and continuously optimizing the layer thickness in different directions.

The above research mainly focuses on the application of response surface method in optimization design, without involving research on dual constraints while requiring lightweight. In the design of transportation packaging boxes, there is a certain compromise between insulation performance and safety factor. On the one hand, excessive lightweight design may result in poor insulation performance, threatening the stability of loads under extreme temperature conditions. On the other hand, excessive emphasis on safety factors may make the box too heavy, increasing transportation costs and difficulties. Therefore, it is necessary to study new design methods and materials to find a more reasonable balance, so that the box can ensure coordinated development of insulation performance and structural safety while being lightweight. This paper aims to explore how to use the response surface algorithm to optimize the design of transportation packaging boxes, meet the requirements of lightweight under the constraints of insulation effect and strength, and find the best combination of design parameters through numerical simulation and multi-objective optimization methods. Firstly, relevant models are established for calculation and

simulation using finite element Ansys software. Secondly, the requirements of insulation conditions and strength constraints are analyzed. Finally, the response surface algorithm is used to simultaneously consider the insulation effect and strength requirements to meet lightweight optimization design.

2. Model Establishment and Numerical Simulation.

2.1. Geometric Model

A certain transportation packaging box is rectangular in shape, with a bell-shaped structure composed of a box cover and a box base, as shown in **Figure 1**(a). The box walls are made of lightweight composite materials sandwiched together. Fiberglass provides the necessary structural strength and rigidity to the transportation packaging box, while also adding insulation functionality. The inner skin is made of 3mm thick aluminum plate, while the outer skin is made of 2mm thick aluminum plate. The combination of these two skins is designed to achieve better insulation. Aluminum square tubes, arranged in a cross pattern, are used as the framework of the box. These tubes are connected by welding, and the outer skin is connected to the box framework by riveting. Insulation material is filled in the gaps between the aluminum square tubes to serve as the insulation layer. A detailed schematic of the box wall structure is shown in **Figure 1**(b).

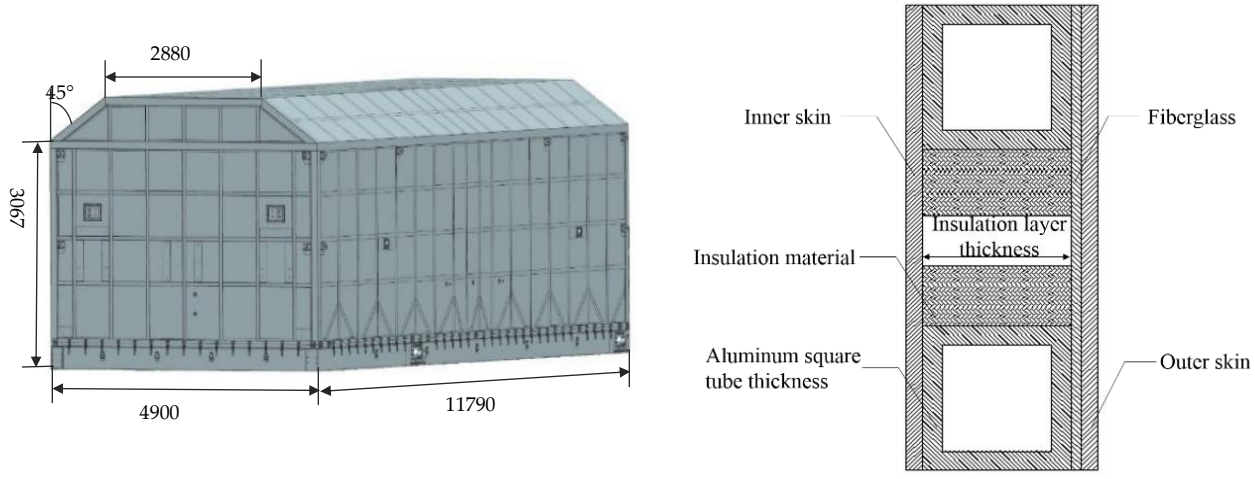

(a) Overall structure of box body (b) Partial enlarged view of box wall structure

Figure 1. Basic structure of transport packing box.

2.2. Numerical Simulation Method

During the heat transfer process in insulation, phenomena such as thermal conduction, thermal convection, and thermal radiation [14] continuously occur, with these mechanisms acting simultaneously. Throughout the heat transfer process, the interior of the transportation packaging box must consistently satisfy conservation equations. This implies that in the insulation system, the mutual influence and synergistic effect of various heat transfer mechanisms are crucial, while also ensuring energy conservation to safeguard the thermal performance and efficiency of the system. The heat transfer across the box wall can be divided into three stages, as shown in **Figure 2**: initially, heat is transferred from the outer side of the box wall through air convection and radiation between the box wall and the external environment; then it is conducted between the box walls through solid conduction to various layers of materials; finally, heat is transferred by air convection and radiation between the box body and the interior of the box.

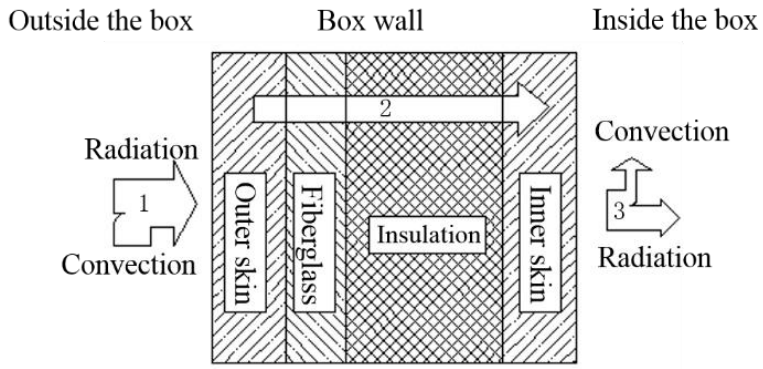

Figure 2. Heat transfer process.

2.2.1. Heat conduction equation

The Fourier heat conduction law is the fundamental law of heat conduction, which can be used to analyze and calculate the heat conduction process inside solid objects. According to this law, the rate of heat conduction is directly proportional to the cross-sectional area and the temperature gradient, while inversely proportional to the material's thermal conductivity [16]. This law provides a fundamental understanding of the mechanisms of heat conduction in solids, offering an important theoretical basis for research and practical applications in the field of thermodynamics. The law illustrates that heat is transferred from regions of high temperature to regions of low temperature, and the rate of conduction is directly proportional to the temperature gradient and inversely proportional to the material's thermal conductivity [17]. The Fourier formula is as follows:

$$q = \frac{\Phi}{A} = -\lambda \frac{dt}{dx} \tag{1}$$

In the equation: Φrepresents the heat flux (W); A represents the heat transfer area (m^2), q represents the heat flux density transmitted along the x-axis direction $(\mathrm{W/m^2})$, λ represents the thermal conductivity of the material $(\mathrm{W/m \cdot}k)$, t represents the temperature (K), x represents the coordinate on the heat transfer surface (m), $\frac{dt}{dx}$ represents the temperature gradient along the x-axis direction (W).

2.2.2. Heat convection equation

Convective heat transfer refers to the process where heat is transferred through the movement of fluid. The rate of convective heat transfer depends on the fluid's flow properties (such as velocity and fluid properties) and the heat transfer coefficient of the transfer surface [18]. When one side of an object is heated, the temperature of the fluid on that side increases, its density decreases, generating buoyancy, which causes the fluid to rise. On the other side, cooling leads to a decrease in fluid temperature, an increase in density, causing the fluid to sink, thus forming a circulating motion of the fluid, thereby achieving the transfer of heat. The formula for the rate of energy transfer in convective heat transfer is as follows:

$$q = h(T_S - T_\infty) \tag{2}$$

In the equation: q represents the heat flux density $(\mathrm{W/m^2})$;h represents the convective heat transfer coefficient (K), T_∞ represents the surface temperature (K).

2.2.3 Thermal radiation equation

Radiative heat transfer refers to the process where heat is transferred through electromagnetic radiation. The rate of radiative heat transfer depends on the temperature and the radiative properties of the surface [19]. The formula for calculating the radiation energy of a substance using the blackbody model is as follows [20]:

$$\phi = \varepsilon A \sigma_b T^4 \quad (3)$$

In the equation:A represents the surface area of the object (m^2);σ_b represents the Stefan-Boltzmann constant σ=5.67*10^{-8}W/$(m^2 \cdot K^4)$; Trepresents the surface temperature of the object (K).

2.3. Establishment of Finite Element Model

In this paper, we will utilize the Ansys finite element analysis method to simulate the structural behavior of the transportation packaging box, especially considering the comprehensive consideration of insulation performance and box weight.

To ensure the reliability and accuracy of the numerical model, mesh independence verification was conducted [21]. Appropriate mesh generation algorithms were employed to ensure sufficient mesh density in the critical areas and structural details of the model. Based on this, a series of mesh refinement and coarsening operations were performed to generate a set of meshes with different densities. Finite element model simulations were then run on each mesh density to obtain corresponding numerical results for each monitoring point, as shown in **Figure 3Figure 3.** Influence of grid size on simulation result..

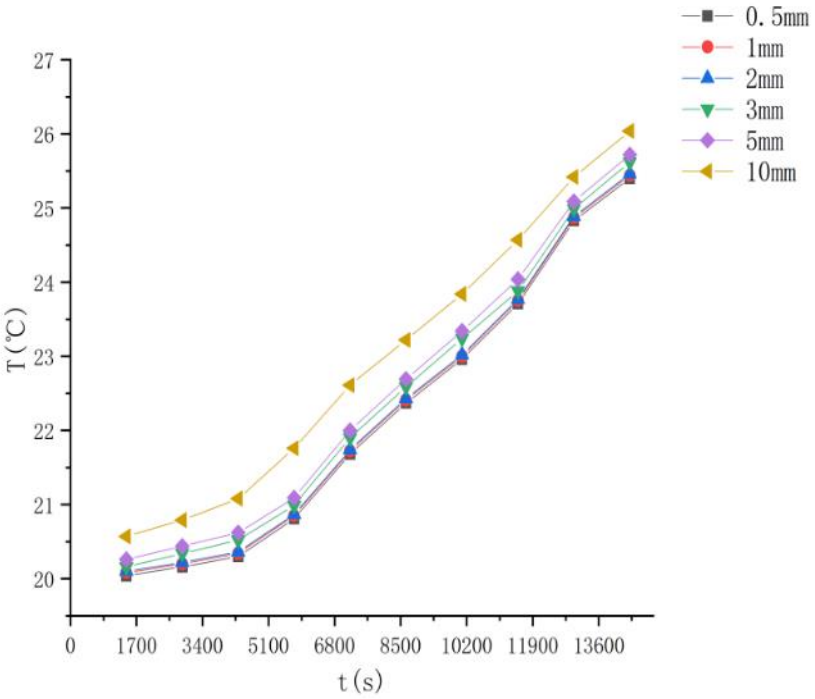

Figure 3. Influence of grid size on simulation result.

From **Figure 3**, it can be clearly observed that: when the mesh size is larger, changing the mesh size significantly affects the simulation results; however, when the size is reduced to 2 mm and continues to decrease the mesh size, the finite element simulation results remain basically unchanged. This indicates that within a larger range of mesh sizes, the choice of mesh has a significant sensitivity to simulation results, while within a smaller size range, further reducing the mesh size has less impact on simulation results. Such observations emphasize the careful selection of mesh size during simulation to ensure the accuracy and reliability of the results. The four main components of the transportation packaging box, including the inner skin, fiberglass, insulation layer, and outer skin, are all structurally regular cuboids. The size of the tetrahedron-dominated mesh, divided using ICEM CFD software, is set to 2 mm. This ensures both mesh quality and computational accuracy. Subsequently, the mesh is imported into FLUENT for result calculation.

3. Response Surface Experimental Design

This chapter aims to clarify the direction and objectives of the research, providing a clear framework for the dual-constrained optimization of insulation performance and material safety factor of the transportation packaging box. Based on the principles of response surface experimental design, a series of experiments covering different values of design parameters will be designed, conducted, and relevant data collected. Utilizing the collected data, a response surface model will be established, which accurately reflects the influence of design parameters.

3.1. Box-Behnken Experimental Design

Response Surface Methodology (RSM) is a method used to construct an approximate model between the objective function and design variables. The corresponding model covers first-order, second - order, and higher-order polynomial models, with the second-order polynomial model being the most widely used. In response surface design, commonly used design methods include central composite design, Box-Behnken design, factorial design, D-Optimal, etc., among which the most common and effective are the central composite design and Box-Behnken design methods [22].

This paper selects the second-order polynomial fitting response surface model and the Box-Behnken method to establish a three-factor three-level response surface model, including the thickness of the insulation material, the thermal conductivity of the insulation material, and the thickness of the aluminum square tube. The response surface model schematic diagram is shown in **Figure 4**.

$$Y = a_0 + \sum_{i=0}^{n} a_i x_i + \sum_{i<j}^{n} a_{ij} x_i x_j + \sum_{i=1}^{n} a_{ii} x_i^2 + \varepsilon \tag{2}$$

In the equation: x_i, x_j represents the influencing factors; a_0, a_i, a_{ij}, a_{ii} represents the unknown coefficients of each term; n represents the number of influencing factors; ε represents error, the unknown coefficients are determined by the method of least squares.

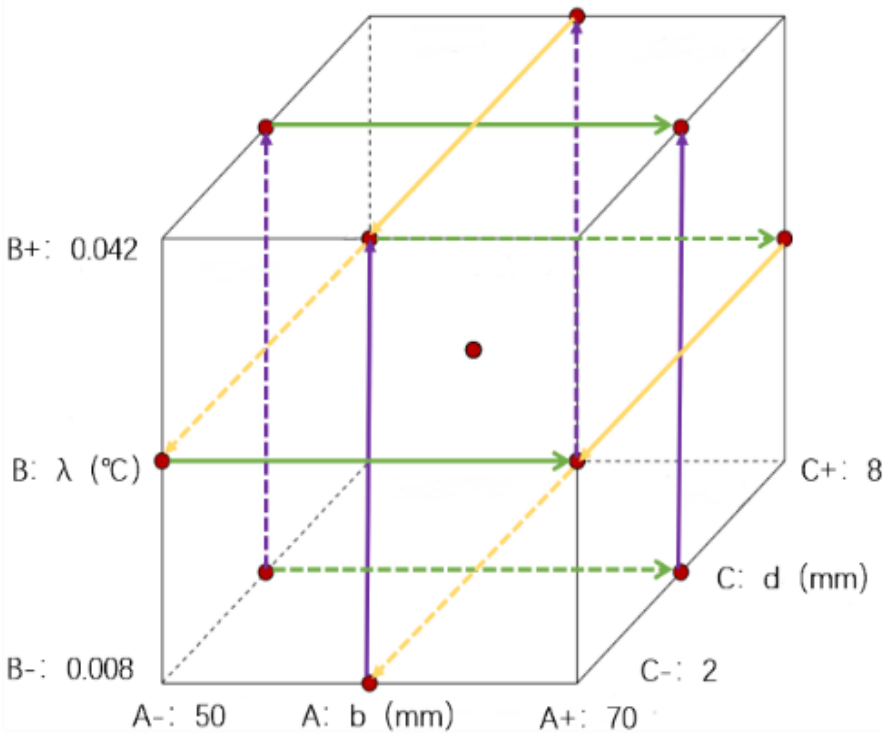

Figure 4. Schematic diagram of Box-Behnken experimental design.

Taking the thickness of the insulation material, the thermal conductivity of the insulation material, and the thickness of the aluminum square tube as three factors, each factor is varied at three levels as shown in **Table 1**.

Table 1. Test factors and levels.

	Level		
Factor	-1	0	1
$b/(mm)$	50	60	70
$\lambda/(W/(m\cdot k))$	0.008	0.025	0.042
$d/(mm)$	2	3.5	5

Using Design-expert software for central composite experiments, finite element numerical simulation experiments were conducted according to the design scheme. The temperature of each monitoring point and the weight of each model were obtained as shown in **Table 2**.

Table 2. Design scheme.

Serial number	b	λ	d	T	S_f	G
1	50	0.025	2	25.72	1.03	119.50
2	60	0.042	5	21.95	1.47	184.50
3	70	0.025	2	25.77	1.27	152.00
4	60	0.025	3.5	23.37	1.24	161.50
5	50	0.025	5	25.27	1.12	138.00
6	70	0.025	5	24.79	1.39	170.50
7	60	0.025	3.5	23.32	1.24	161.50
8	60	0.042	2	23.61	1.36	156.00
9	70	0.008	3.5	20.77	1.21	210.00
10	60	0.025	3.5	23.40	1.24	161.50
11	60	0.025	3.5	23.28	1.24	161.50
12	60	0.008	2	23.01	1.07	189.00
13	50	0.042	3.5	25.61	1.19	147.50
14	70	0.042	3.5	23.24	1.54	192.50
15	60	0.025	3.5	23.30	1.24	161.50
16	50	0.008	3.5	23.86	1.08	164.50
17	60	0.008	5	21.90	1.11	204.50

3.2. Constraint

3.2.1. Safety factor of the material

The structural strength refers to the maximum stress or deformation that structural materials can withstand when subjected to loads, while the safety factor of the material is an indicator of whether the structural material is sufficiently strong [23]. By comparing actual loads or stresses with the ultimate performance of materials or structures, the safety factor helps to address uncertainties, risks, and variations, thereby ensuring that the designed and manufactured products or structures can operate normally under various conditions [24]. The safety factor is a ratio, usually denoted as (Safety Factor), and it is the ratio between the ultimate strength of the material and the actual stress. If is greater than 1, it indicates that the structure is sufficiently safe; if is less than 1, it may require redesign or selection of stronger materials [26]. The definition of the safety factor is as follows:

$$S_f = \frac{S_u}{S_a} \tag{5}$$

Determining the safety factor requires comprehensive consideration of multiple factors, including load, mechanical properties of the material, differences between experimental and design values, calculation models, and construction quality parameters. By consulting literature, the main properties of the box wall material include tensile strength, compressive strength, shear strength, etc. The main material properties of the box wall are shown in **Table 3Table 3.** Materials performance..

Table 3. Materials performance.

	Aluminum	Fiberglass	EPP	XPS	VIP
Tenile strength	450	700	1	0.8	0.4
Compressive strength	350	400	1	0.8	0.4
Shear strength	180	120	0.5	0.5	0.4
Young's modulus	6.9*104	5*104	1500	1500	1000
Poisson's ratio	0.35	0.3	0.3	0.3	0.5

The box is subjected to a wind speed of 20 m/s in the air, and according to the calculation formula for wind pressure and wind speed, the approximate pressure applied is about 245 Pa. Loading and constraints are shown in **Figure 5**. The safety factor is calculated using finite element analysis software by importing the geometric model of the transportation packaging box and assigning appropriate physical and mechanical properties to the box material, such as elastic modulus, Poisson's ratio, tensile strength, compressive strength, shear strength, and the applied load. Through verification analysis of packaging boxes made of different materials, it is found that all three types of materials meet the requirements.

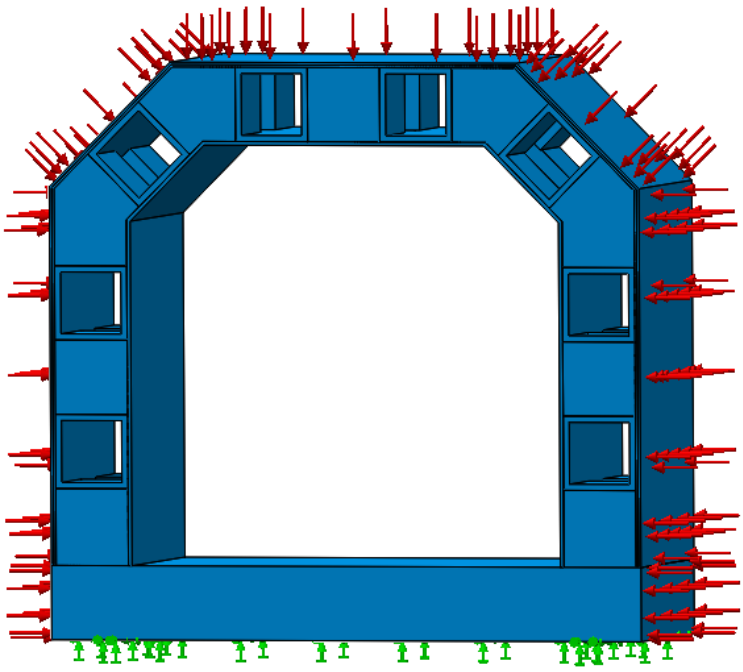

Figure 5. Apply load and constraint.

3.2.2. Thermal insulation performance

The thermal insulation performance of the box is influenced by multiple factors, including the thermal conductivity of composite materials, the thickness of the insulation layer, and the structure of the box. With an external ambient temperature of 32 °C and an initial temperature inside the box of 20 °C, after 4 hours of transportation, the temperature at monitoring points inside the box is checked. The temperature change should not exceed

6 °C to meet design requirements. In this study, the thickness of the insulation material, the thermal conductivity of different insulation materials, and the thickness of aluminum square tubes are considered as three factors affecting thermal insulation performance. An increase in the thickness of the insulation material leads to a decrease in temperature gradient, resulting in a more uniform temperature distribution on the surface of the insulation material. Increasing thickness prevents heat from escaping from the inside to the external environment. High-quality insulation material with lower thermal conductivity reduces the temperature gradient, effectively slowing down the rate of heat conduction and providing better insulation. The thickness of aluminum square tubes not only affects the stability of the structure but also affects temperature transfer; a greater thickness results in a more stable structure. The effects of these three factors on thermal insulation performance are shown in **Figure 6**.

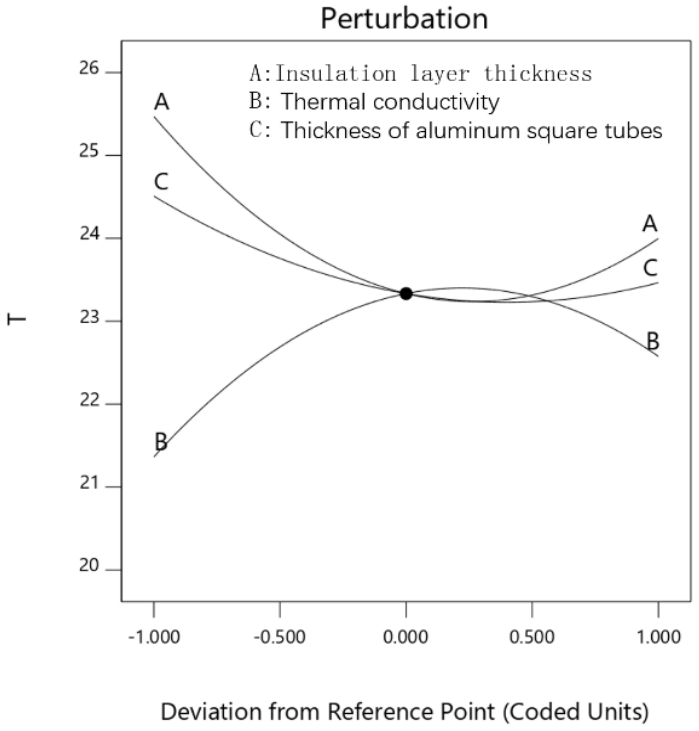

Figure 6. Temperature disturbance diagram.

The perturbation plots shown in Figure 6 illustrate the effects of three factors on temperature. These plots demonstrate how temperature varies as a single factor is moved from the selected reference point while keeping the other factors at their reference values. Flatter lines in the plot indicate that temperature is less sensitive to that factor, while steeper lines indicate greater sensitivity. Therefore, from the plot, it can be observed that there is an inverse relationship between the thickness of the insulation layer and the thickness of aluminum square tubes with the thermal conductivity. The temperature inside the packaging box is more sensitive to changes in the thickness of the insulation layer.

3.3. Optimization Objective

The lightweighting of the spacecraft transportation packaging box is the optimization objective of this paper. The weight of the box is closely related to the choice of materials, as different materials have different densities and strengths, thus selecting different materials will directly affect the weight of the box. The structural design of the box will also impact its weight. A rational structural design can reduce the weight of the box by ensuring strength while minimizing the unnecessary use of materials. The density of the materials constituting the box is shown in **Table 4**.

Table 4. Materials density.

	Aluminum	Fiberglass	EPP	XPS	VIP
Density (Kg/m^3)	2700	1690	67.5	35	100

The mathematical model for optimization design is as follows:

The objective function: Min(G)

The constraint conditions: $\begin{cases} S_f > 1 \\ T \leq 26℃ \\ 50 \leq b \leq 70 \\ 0.008 \leq \lambda \leq 0.042 \\ 2 \leq d \leq 5 \end{cases}$.

4. Results and Discussion

4.1. Establishment and Significance Analysis of Response Equations

Based on the experimental results in **Table 2**, data processing was conducted using multiple quadratic regression fitting, obtaining mapping relationships that accurately describe the parameters' influence on weight.

$$G = 161.5 + 19.44b - 10.94\lambda + 10.13d - 0.13b\lambda + 3.25\lambda d - 10.69b^2 + 27.81\lambda^2 - 5.81d^2 \quad (6)$$

A regression model regarding weight values was established, and the model underwent variance analysis. The F-value of the weight value regression model was 51.13, indicating that the predictive model is highly significant. The probability of obtaining such a large F-value under noise interference is only 0.01%. However, the lack-of-fit test value F=1.15 suggests that the model is not significantly different from pure error misfit. These statistical results emphasize the significance of the predictive model and provide an evaluation of the overall adaptability of the model, thereby offering strong support for the reliability of the model.

Each data point in **Figure 7** represents a specific set of experimental results. In **Figure 7** (a), the external residuals of all data exhibit a linear relationship with the normal probability, indicating that the residuals follow the law of normal distribution, and the data points conform to a normal distribution. In **Figure 7** (b), the distribution of external residuals of all sample points falls within the range of ± 4.81, and no abnormal data points are observed, indicating a normal distribution of the data. Through the analysis in **Figure 7** (c), the predicted values of the internal temperature and the actual values are essentially on the same line, indicating that the model has good accuracy. These results reinforce trust in the model, validating its reliability in prediction and optimization.

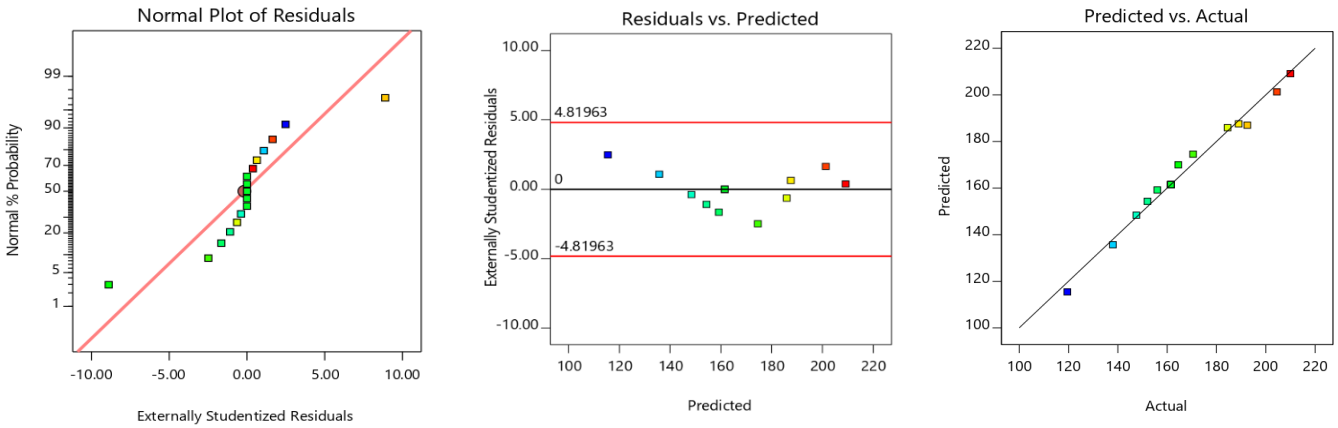

(a) Residual normal probability distribution. (b) Residual and predicted values. (c) Test value and predicted value.

Figure 7. Diagnostic diagram of regression model of temperature value.

4.2. Response Surface Results Analysis

The Box-Behnken method was employed for response surface experimental design, and a quadratic polynomial response surface model was fitted to optimize the parameters under study. During the model validation stage, cross-validation was utilized to ensure the accuracy of the model predictions. Through response surface optimization, we obtained the optimal parameter combination and plotted three-dimensional surface plots illustrating the interaction effects of the three factors on the weight of the transportation packaging box. The surface plots and contour plots provide a visual representation of the impact of various factor variations on weight, as shown in **Figure 8**.

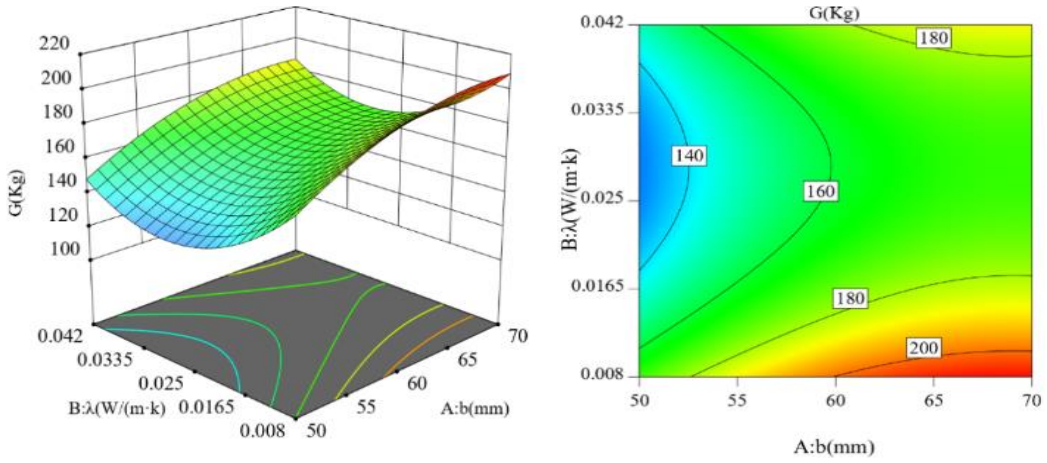

(a) x, λ Interaction

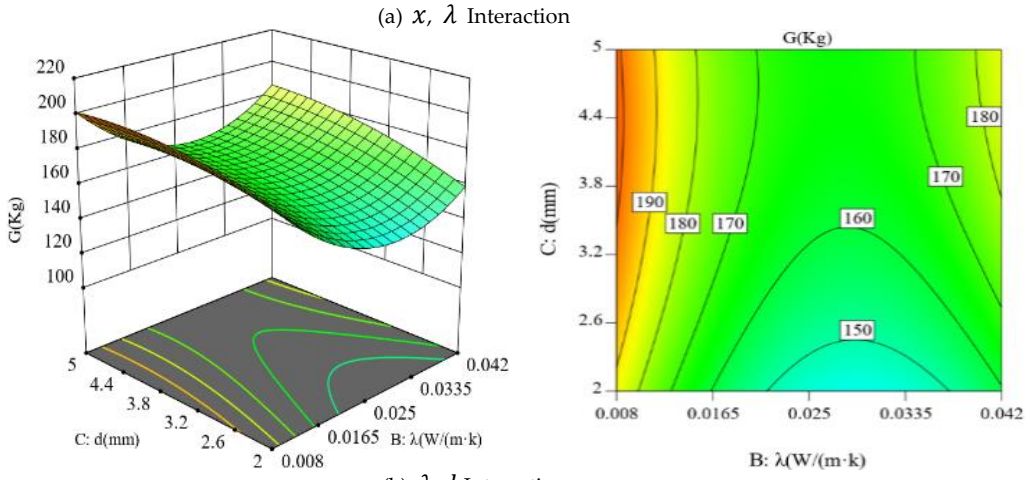

(b) λ d Interaction

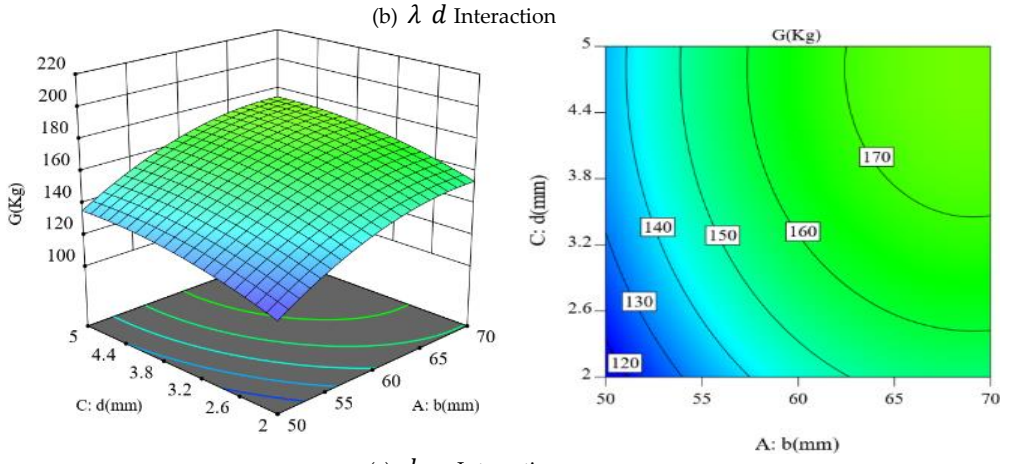

(c) d, x Interaction

Figure 8. Influence of factor interaction on thermal insulation effect.

The shape and variations of the 3D surface in **Figure 8** intuitively demonstrate the significant and complex effects of factor interactions. As shown in **Figure 8** (a), increasing the thickness of the insulation layer increases the amount of insulation material used, thereby increasing the weight of the box and its insulation performance. Choosing insulation materials with lower thermal conductivity not only reduces heat conduction to improve insulation effectiveness, but also increases the overall weight due to the relatively higher density of materials with lower thermal conductivity. From **Figure 8** (b), it can be observed that increasing the thickness of the aluminum square tube also increases the overall weight. However, when the thickness of the aluminum square tube remains constant, changing the material of the insulation layer results in a significant change in the weight of the box. As indicated in **Figure 8** (c), the interaction between insulation materials of different densities and the thickness of the aluminum square tube is noticeable. When the density of the insulation material remains constant, changing the thickness of the aluminum square tube has a more pronounced effect on the overall weight of the box.

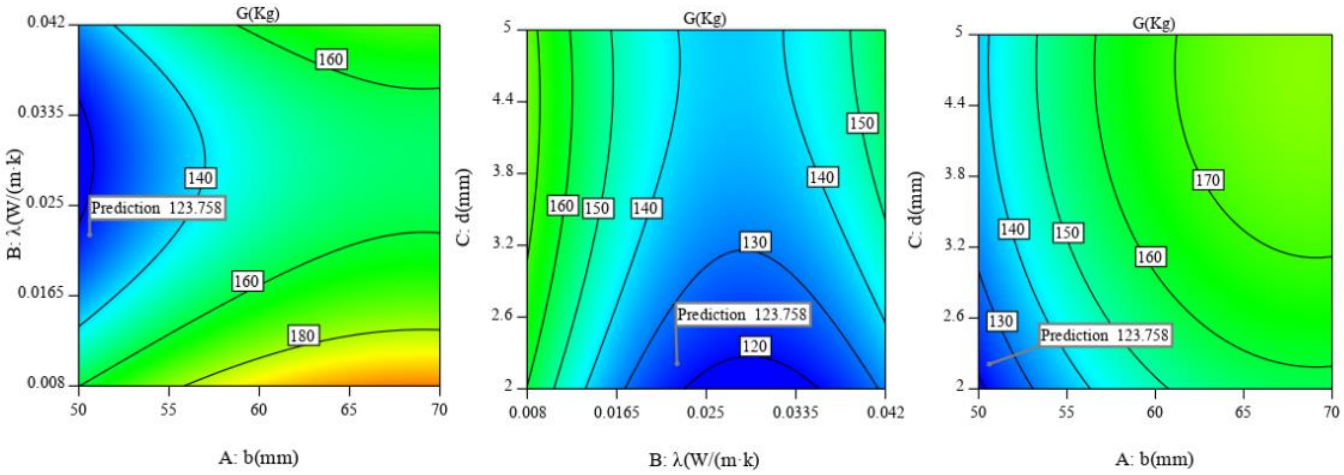

Figure 9. Optimal solution.

Based on the optimization analysis and **Figure 9**, the optimal values for lightweight optimization design are obtained as follows: insulation layer thickness b=52.16 mm, aluminum square tube thickness d=2.23 mm, and the material adopted is Vacuum Insulation Panel (VIP). Under these conditions, the weight of the transportation packaging box reaches 123.76 units. The optimization effect is significant, reducing the weight of the box by 13.3% compared to the original design, indicating a rather ideal weight reduction outcome.

5. Conclusion

This paper utilizes the response surface optimization method to analyze and optimize the weight of the spacecraft transport packaging box. The influences of factors such as the thickness of insulation materials, the type of insulation materials, and the thickness of aluminum tubes are analyzed and verified. Additionally, the effect of the material safety factor on structural stability is analyzed, and conclusions are drawn based on the overall weight analysis:

(1) Utilizing the tensile, compressive, and shear strength of materials to analyze the material safety factor, which represents the ratio between the material's ultimate strength and the actual stress. A safety factor greater than 1 indicates that the structure is sufficiently safe. Analysis reveals that the optimized structure of the spacecraft transport packaging box has a safety factor of 1.21 under corresponding operating conditions, meeting the requirements for strength and stability.

(2) The thickness of the insulation material, the thermal conductivity of the insulation material, and the thickness of aluminum tubes are not only evaluation indicators for lightweighting of the box but also three crucial factors affecting insulation performance. Finite element analysis indicates that under the influence of these factors, the internal temperature of the spacecraft transport packaging box does not exceed 26°C after 4 hours, meeting the expected requirements.

(3) The response surface algorithm provides a powerful tool for box design, applicable to various design variables and constraints. Through the optimization design considering the box material, insulation performance, and material safety factor, the lightweighting of the transport packaging box is achieved while maintaining excellent insulation performance and meeting strength requirements.

References

1. Li, B., Huang, Xiu., Shen, L. Optimal design case of transport package. Packaging Engineering, 2016, 37(21), 137-141. https://doi.org/10.19554/j.cnki.1001-3563.2016.21.025
2. Ma, X., Zhang, L., Wang, X., et al. Simulation analysis and optimization design of temperature field of used lithium battery transport packaging boxes for vehicles. Packaging Engineering, 2024, (13), 300-30. https://doi.org/10.19554/j.cnki.1001-3563.2024.13.035
3. Tserpes, K., Sioutis, I. Advances in composite materials for space applications: A comprehensive literature review. Aerospace. 2025; 12(3), 215. https://doi.org/10.3390/aerospace12030215
4. Shi, W., Gao, F., Chai, H. Application and prospect of composite materials in spacecraft structure. Aerospace Materials & Technology, 2019, 49(04), 1-6. https://doi.org/10.12044/j.issn.1007-2330.2019.04.001
5. Xiao, G., Hao, W., Zhang, G., et al. The development of containers for air transport of spacecraft and an evaluation. Spacecraft Environment Engineering, 2010, 27(06), 795-799. https://doi.org/10.3969/j.issn.1673-1379.2010.06.027
6. Su, X., Fu, S., Pei, Y. Analysis of passive thermal insulation performance of packaging box for spacecraft transportation. Journal of Astronautics, 2012, 33(09), 1334-1340. https://doi.org/10.3873/j.issn.1000-1328.2012.09.021
7. Singh, S. P., Burgess, G., Singh, J. Performance comparison of thermal insulated packaging boxes, bags and refrigerants for single-parcel shipments. Packaging Technology and Science: An International Journal, 2008, 21(1), 25-35. https://doi.org/10.1002/pts.773
8. Paquette, J., Mercier, S., Marcos, B., et al. Modeling the thermal performance of a multilayer box for the Transportation of perishable food. Food and Bioproducts Processing, 2007, 105, 77-85.5 https://doi.org/10.1016/j.fbp.2017.06.002
9. Rezgar, H., Taher, A., Ali, D., Richard, E. L. Thermal conductivity of low density polyethylene foams Part I: Comprehensive study of theoretical models. Journal of Thermal Science, 2019, 28(04), 745-754. https://doi.org/10.1007/s11630-019-1135-3
10. Matsunaga, K., Burgess, G., Lockhart, H. Two methods for calculating the amount of refrigerant required for cyclic temperature testing of insulated packages. Packaging Technology and Science: An International Journal, 2007, 20(2), 113-123. https://doi.org/10.1002/pts.747
11. Liu, C., Zhang, S., Zhou, H., et al. Structural optimization of portable cold storage incubator. Journal of Jilin Institute of Chemical Technology, 2011, 28(01), 29-33. https://doi.org/10.16039/j.cnki.cn22-1249.2011.01.017
12. Ao, F., Huo, W., Zhu, G., et al. Lightweight design of variable cross-section column of high-rise stacker based on response surface method. Hoisting and Conveying Machinery, 2023, (11), 58-66.
13. Huang, D., Wang, J., Lin, G., et al. Research on lightweight of long gauge aluminum alloy van semitrailer based on adaptive response surface methodology. Aluminum Fabrication, 2023, (01), 64-72. https://doi.org/10.3969/j.issn.1005-4898.2023.01.13
14. Wu, S., Guo, J., Li, Z., et al. Structural Analysis and Optimization Design of Bucket-Wheel Body of Bucket-Wheel stacker/reclaimer. Machinery Design & Manufacture, 2014, (11), 5-8. https://doi.org/10.19356/j.cnki.1001-3997.2014.11.002
15. Liu, B., Haftka, R. T., Akgün, M. A. Two-level composite wing structural optimization using response surfaces. Structural and Multidisciplinary Optimization, 2000, 20(2), 87-96. https://doi.org/10.1007/s001580050140
16. Wan, C., Duan, S., Nie, X., et al. Research on finite element numerical simulation method of large aviation structure. Mechanical Science and Technology for Aerospace Engineering, 2018, 37(05), 816-820. https://doi.org/10.13433/j.cnki.1003-8728.20180021
17. Linde, P. Virtual testing of Stiffened Composite Panels at Airbus. International Journal of Structural Stability & Dynamics, 2010, 10(04), 589-600. https://doi.org/10.1142/S0219455410003634
18. Sun, M., Liu, X., Jiang, S. Numerical simulation of boundary layer on graded grid by multiscale finite element method. Journal of Yangzhou University (Natural Science Edition), 2021, 24(04), 5-10. https://doi.org/10.19411/j.1007-824x.2021.04.002
19. Luo, D. Research on optimal design of temperature-controllable packing box based on temperature field simulation. Tianjin, Tianjin University of Science and Technology, 2020. https://doi.org/10.27359/d.cnki.gtqgu.2020.000201
20. Wang, D. Analysis of heat conduction based on Fourier law. Scientific and Technological Innovation, 2019(13):45-46.
21. Yang, Z., Wu, X., Lan, M. Research on the design of high temperature work clothing based on Fourier Law. Scientific and Technological Innovation, 2020, (22), 192-193.

22. Ma, Y., Chen, A., Deng, C. A multiscale mesh generation method for textile composite. Acta Aeronautica et Astronautica Sinica, 2024, 45(10), 429180. https://doi.org/10.7527/S1000-6893.2023.29180
23. He, Y., Wang, Y., Zhang, D., et al. Optimization design for turbodrill blades based on a twisting method. Journal of Petroleum Science and Engineering, 2021, 205, 108892. https://doi.org/10.1016/j.petrol.2021.108892
24. Cheng, X., Zhang, J., Li, Z. Engineering implication of load safety factor in aircraft structure design. Mechanics in Engineering, 2021, 43(04), 599-602. https://doi.org/10.6052/1000-0879-20-275
25. Li, B., Zhu., Bu, K., et al. Research on design method of reliability safety factor of spacecraft structure. Structure & Environment Engineering, 2018, 45(04), 23-30. https://doi.org/10.19447/j.cnki.11-1773/v.2018.04.004
26. Solazzi, L., Vaccari, M. Reliability design of a pressure vessel made of composite materials. Composite structures, 2022, 279, 114726. https://doi.org/10.1016/j.compstruct.2021.114726